Theoretical Study of Quinoline Aza Oxa Thia 17-Crown -6 Complexes: NICS Aromaticity

Nosrat Daryapour,* Roya Afsharpour, Esmael Rostami *

Department of chemistry, Payame Noor University, PO BOX 19395-3697 Tehran, Iran.

e.rostami@pnu.ac.ir

Abstract

Complexation of quinoline aza oxa this 17-crown-6 (**L**) with some metal cations (K^+, Na^+, Li^+, Mg^{2+}) was studied through computational methods. Hartree-Fock method was employed to identify structure and thermodynamical binding constant of crown and metal ions complexes. The calculations were conducted at the HF/6-31g and HF/Lanl2DZ levels of theory. According to the obtained data Mg^{2+} ion formed the most stable complex with crown and equilibrium binding constants of complex formation has the following order: L. K^+ < L. Na^+ <L. Li^+ <L. Mg^{2+}. In order to verify the physical properties of free crown and complexes some important physical properties including band gap, energy, hardness and dipole moments were obtained and discussed. The electron distribution over the free crown and its L. Mg^{2+} complex was studied which showed that in the free crown and its L. Mg^{2+} complex, Highest Occupied Molecular Orbital (HOMO) were distributed mainly over the sulfur atom. For both of them Lowest Unoccupied Molecular Orbital (LUMO) were distributed over aromatic rings. HOMO and LUMO orbitals in L. Mg^{2+} complex was not distributed over Mg^{2+} ion and the ion remained bare. Also, atomic charges and charge transfer between donors and acceptors were studied using natural bond orbital analysis (NBO). The charge of Mg^{2+} ion in the complex is 1.69095 e. In order to study the effect of complex formation and structural changes on the aromaticity of rings, Nuclear Independence Chemical Shift (NICS) and aromaticity were obtained and discussed.

Keywords Quinoline, Aza Oxa This 17–Crown–6, NICS (0) Aromaticity, Metal Ion Complex, Theoretical Study

Introduction

The first reported crown ethers were prepared by Pedersen in 1967 and their host-guest properties toward metal ions were identified [1]. The supramolecular properties of crown ethers were enhanced by several structural modifications such as application of softer donor atoms, especially nitrogen and sulfur in the cavity of crown ether [2], insertion of side chains (lariats) [3] in the crown ether structure and synthesis of three-dimensional macrocycles [4].

Supramolecular chemistry has been developed into new fields due to the mentioned changes in the macrocycles and similar structures as major building blocks of supramolecular assemblies [5-7]. In this content, plenty of applications have been explored for the wide range of macrocyclic architectures [8,9]. They have also played a significant role in the synthesis and study of challenging molecular architectures [10]. Self-assembly of macrocycles is an important tool for the construction of supramolecular arrays such as nanostructures [11]. In fact, construction of supramolecular systems occurs through host-guest or similar interactions [12].

In continuation of our researches on the synthesis and application of crown ethers and their derivatives [13], in this research computational study of metal ion complexation of 17-crown–6 containing quinoline was reported.

Computational Methods

Gaussian 09 software package was utilized to calculate the structures and properties of the system [14]. GussView 5 was also used to construct input files and observe the output files [15]. At first, a crown (**L**) was optimized using semi-empirical methods (PM6) and the frequency calculation shows that the first frequency mode is positive and there are no imaginary structures. Aza oxa thia crown structure and complexes were optimized using HF/6-31g and HF/Lanl2DZ levels of theory. DFT calculations led to the destruction of molecules,

thus we continue calculations using HF methods. Energy minima without imaginary frequencies confirmed the accurate calculations. Physical properties were obtained using optimized computation and frequency calculations. HOMO and LUMO orbitals of crown and Mg^{2+} complex was obtained using output files. The natural bond orbital analysis was performed using Mg^{2+} complex output. NICS aromaticity of aromatic rings in free crown and complexes were also attained using optimized structures.

Results and Discussion

Figure 1 shows the structure for crown (**L**). At first, crown (**L**) was optimized using semi-empirical methods (PM6) and the frequency calculation shows that the first frequency mode is positive with no imaginary structures. Then, crown (**L**) and its metal ion complexes were optimized using the Hartree-Fock method with HF/6-31g and HF/Lanl2DZ methods and basis sets. The calculated physical properties are summarized in Table 1. Total energy, dipole moments and frontier orbitals energies (HOMO and LUMO) were extracted from output files. The hardness and polarizability as well as bandgap were calculated according to the following equations.

For investigating the theoretical calculation of polarizability, the mean diagonal polarizability on the main axes was calculated as the polarizability.

$\alpha = (1/3)\ (\alpha_{XX}+\alpha_{YY}+\alpha_{ZZ})$

More polarizability reflects less stability of a molecule or complex [16]. The bandgap is the difference between HOMO and LUMO orbitals. The higher band gaps between frontier orbitals show the more stability of the molecule or complex [17].

$\text{Bandgap} = E_{LUMO} - E_{HOMO}$

According to the following equation, hardness (η) is attained using ionization potential and electron affinity. The ionization potential and electron affinity could be obtained from the HOMO and LUMO energies [18].

$\eta = (IP - EA)/2 = (E_{LUMO}-E_{HOMO})/2$

$EA = -E_{LUMO} \quad IP = -E_{HOMO}$

The energy of crown (**L**) and its metal ion complexes are reported in Table 1 and Figure 2. According to the data reported energy increases with the following order: L. Mg2+<L.Na^+<L.Li^+<L^a<L.K^+<L^b. Mg^{2+} complex of crown (**L**) has the lowest energy and, as basis set comparison point of view, energy according to Lanl2DZ basis set is higher compared to 6-31g basis set for the crown (**L**). Based on the Bandgap, hardness of crown ether (**L**) and its metal ions complexes are appeared in Figure 3. According to Figure 3 and Table 1, the order of band gap is L. Na+>L.Li^+>L^a>L^b>L.Mg^{2+}>L.K^+ and hardness order is L. Na+>L.Li^+>L^a>L^b>L.Mg^{2+}>L.K^+. Band gaps of L. Na^+ and L. K^+ complexes are strongly smaller than those of other band gaps. The hardness of complexes is approximately similar to crown (**L**) (Figure 3). Similar to other physical properties, dipole moments of crown (**L**) and complexes are reported in Table 1 and Figure 4. According to the data, the orders of dipole moments are: L. Mg2+>L.Li^+>L.Na^+>L.K^+>L^a>L^b. The calculated dipole moment of L. Mg^{2+} complex is the highest. The dipole moment of crown (**L**) obtained from Lanl2DZ basis set is higher compared to 6-31g basis set.

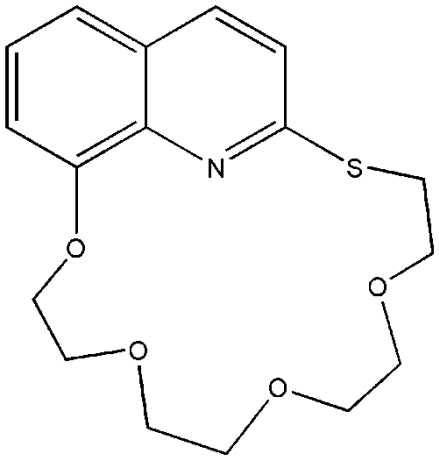

Figure 1: Crown ether (L) structure

Table 1: Calculated physical properties of crown (L) and its metal ion complexes

Row	Entry	Energy/A.U.	E_{HOMO}/ev	E_{LUMO}/ev	Band Gap/ev	Dip. Mom./D.[c]	Hard.[d]
1	L[a]	-1406.87919474	-0.29640	0.08326	0.37966	3.9717	0.18983
2	L[b]	-1019.41951892	-0.30009	0.07216	0.37225	3.9354	0.186125
3	L.Li[a]	-1414.32047006	-0.40936	-0.02749	0.38187	5.2391	0.190935
4	L.Na[a]	-1568.68989017	-0.41204	-0.02935	0.38269	5.1302	0.191345
5	L.K[b]	-1047.20144687	-0.42378	-0.07305	0.35073	4.4887	0.175365
6	L.Mg[a]	-1606.23015487	-0.53916	-0.16726	0.3719	6.7447	0.18595

a: HF/6-31g, b: HF/Lanl2DZ, c: Dipole Moments/Debye, d: Hardness

Dipole moments L. Mg2+>$L.Li^+$>$L.Na^+$>$L.K^+$>L

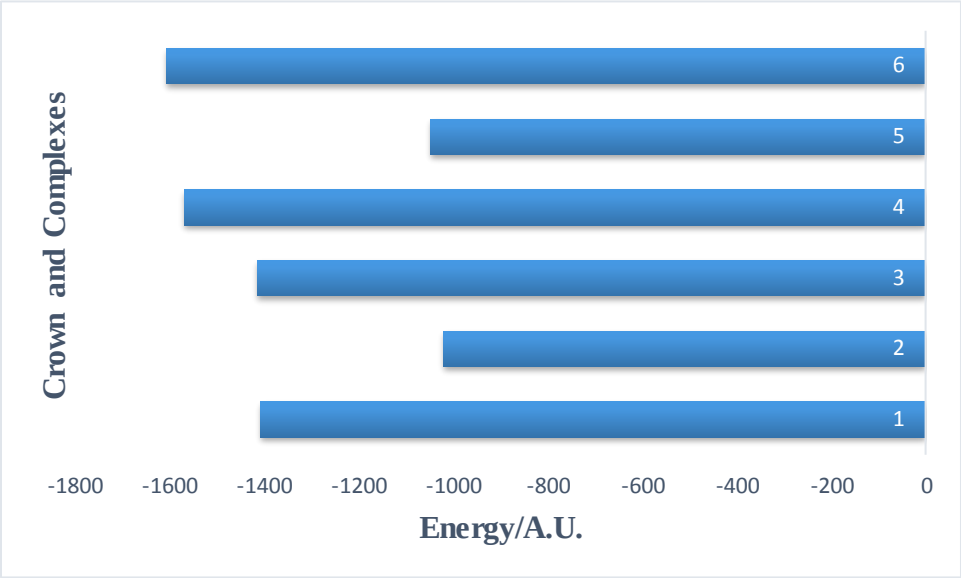

Figure 2: Energy of crown (L) and its metal ion complexes

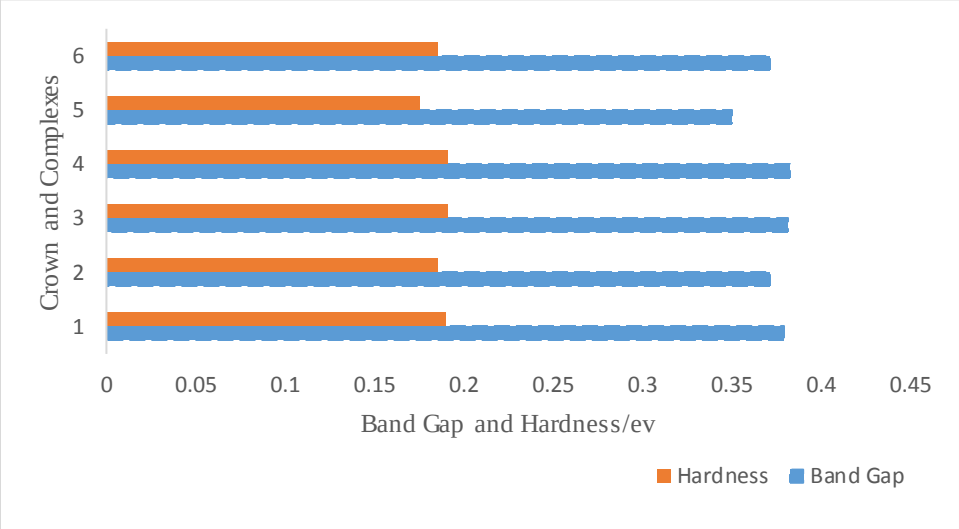

Figure 3: Band Gap and Hardness of crown (L) and its metal ions complexes

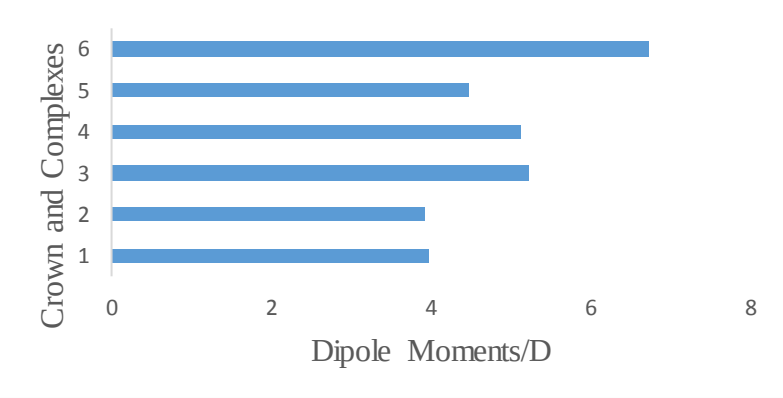

Figure 4: Dipole moment of crown (L) and its metal ion complexes

Table 2: Thermal properties (ΔH and ΔG) of crown (L) and its complexes

Entry	ΔH, Hartree/Part.d	ΔG, Hartree/Part.
L.HF [a]	-1406.465449	-1406.534680
L.HF[b]	-1019.006011	-1019.075628
$L.Li^{+a}$	-1413.902151	-1413.971637
$L.Na^{+a}$	-1568.272925	-1568.345551
$L.K^{+b}$	-1046.785086	-1046.861508
$L.Mg^{2+a}$	-1605.810973	-1605.878728
Li^{+a}	-7.233120	-7.248228
Na^{+a}	-161.656916	-161.673705
K^{+b}	-27.703345	-27.720882
Mg^{2+a}	-198.809349	-198.826198

a: HF/6-31g b: HF/Lanl2DZ

Table 3: Thermal properties (ΔH and ΔG) of complex formation reactions

Entry	ΔΔH, Hartree/Part.[c]	ΔΔG, Hartree/Part.	ΔΔH, Kcal/mol	ΔΔG, Kcal/mol	K_f	$LogK_f$
$L.Li^{+a}$	-0.203582	-0.188729	-127.749	-118.429	6.445×10^{86}	86.809
$L.Na^{+a}$	-0.15056	-0.137166	-94.478	-86.073	1.236×10^{63}	63.092
$L.K^{+b}$	-0.07573	-0.064998	-47.521	-40.787	7.893×10^{29}	29.897
$L.Mg^{2+a}$	-0.536175	-0.51785	-336.455	-324.955	1.564×10^{238}	238.194

a: HF/6-31g b: HF/Lanl2DZ c: Hartree/Particle = 627.509 Kcal/mol

$L.K^{+} < L.\ Na^{+} < L.\ Li^{+} < L.\ Mg^{2+}$

Based on the data reported in Tables 2 and 3, formation constants of complexes showed the following order $L.\ K^{+} < L.\ Na^{+} < L.\ Li^{+} < L.\ Mg^{2+}$. Mg^{2+} ion, with the crown (**L**) forming the most stable complex. Complex formation between crown and metal ions depends on the temperature, size of crown ring, radius of metal ion, types of donors in crown ring and molecule, charge of metal ion, solvent and three-dimensional structure of crown. In Fig. 5, the optimized structure of **L** using HF method is appeared and in Figure 6 to Figure 9 from two sides, the optimized structures of metal ions complexes with **L** are also reported.

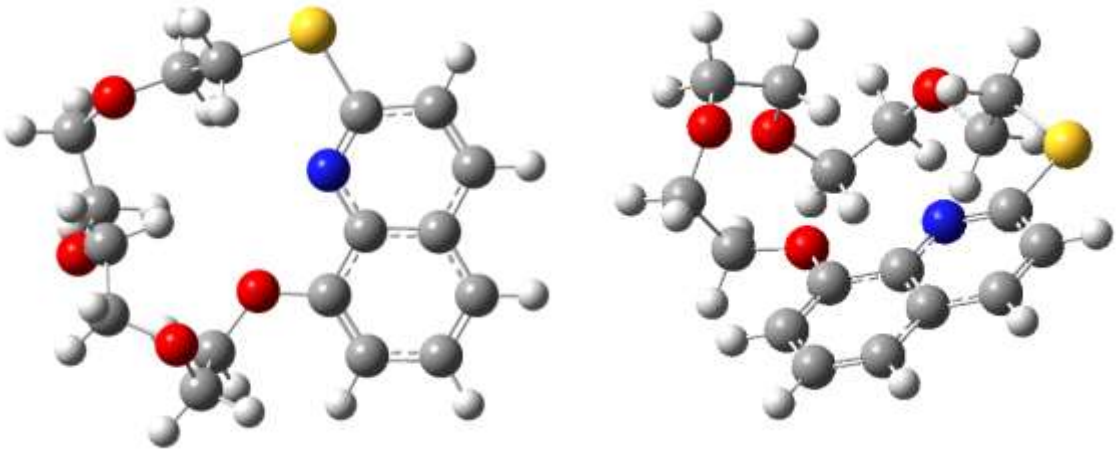

Figure 5: The calculated 3D structure of crown ether (L) from two sides using HF/6-31g

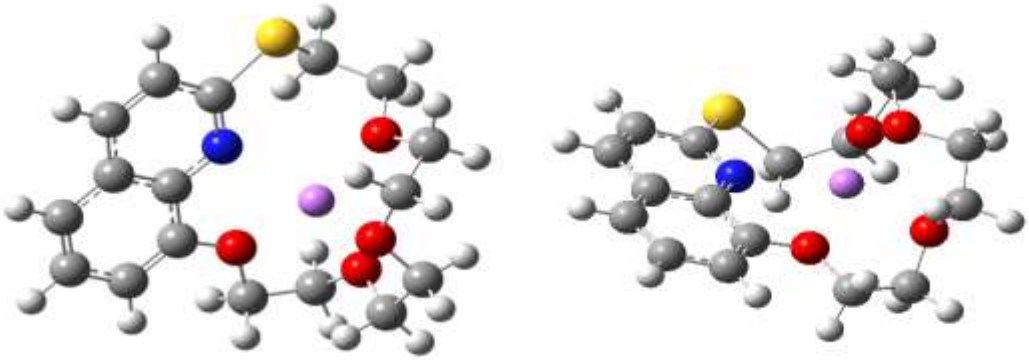

Figure 6: The calculated 3D structure of Li^+ complex with crown ether (L) from two sides

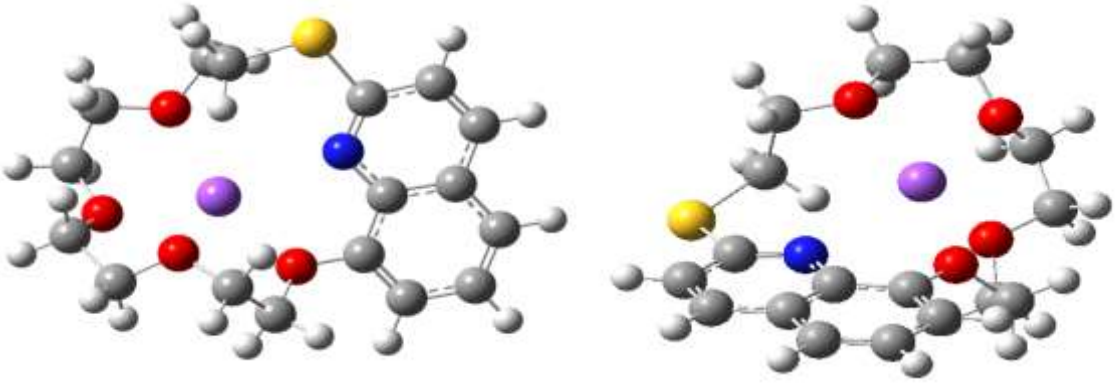

Figure 7: The calculated 3D structure of Na^+ complex with crown ether (L) from two sides

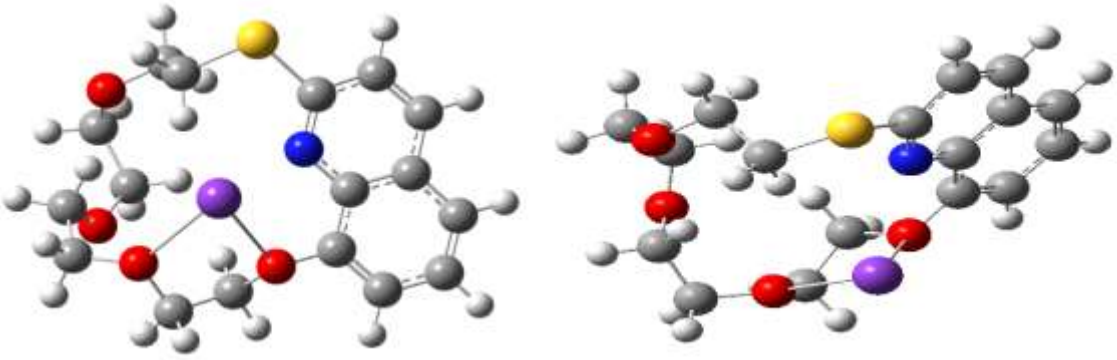

Figure 8: The calculated 3D structure of K^+ complex with crown ether (L) from two sides

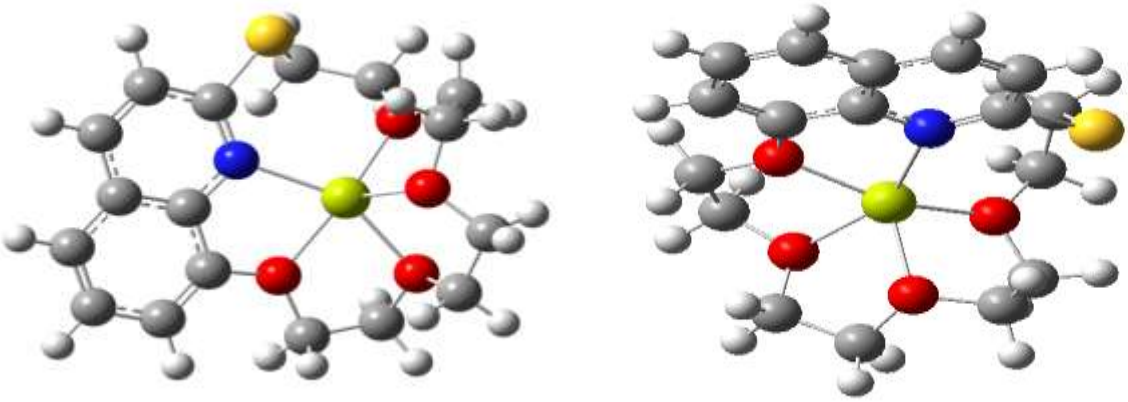

Figure 9: The calculated 3D structure of Mg^{2+} complex with crown ether (L) from two sides

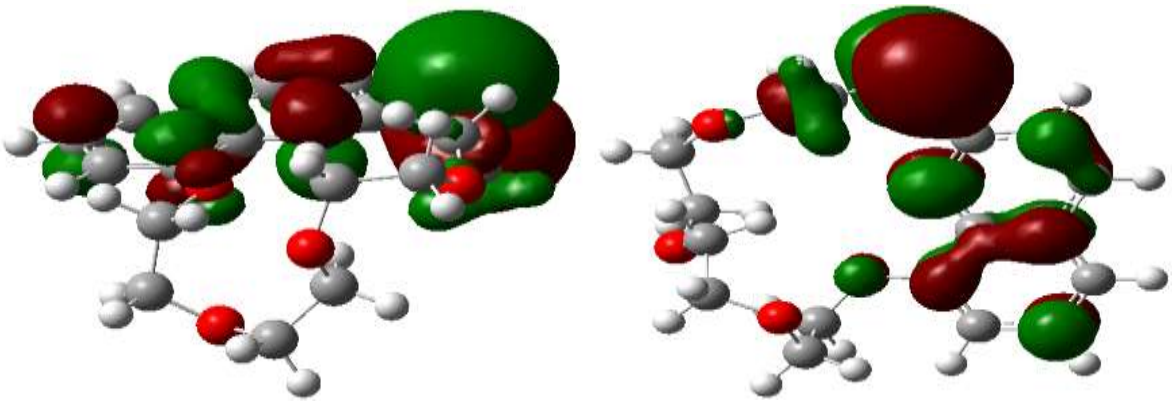

Figure 10: HOMO orbital of crown ether (L) from two sides

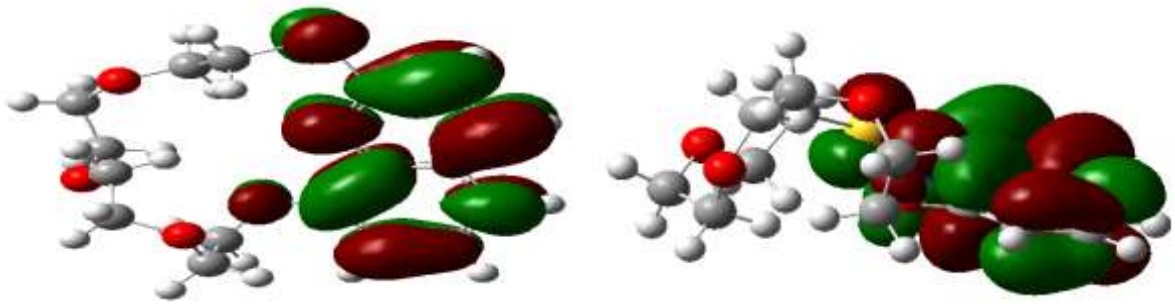

Figure 11: LUMO orbital of crown ether (L) from two sides

HOMO and LUMO orbitals of crown (**L**)-Mg^{2+} complex is reported in Figures 12 and 13. The HOMO orbital is strongly distributed on sulfur atom; while the LUMO orbital was extensively distributed on the quinoline ring.

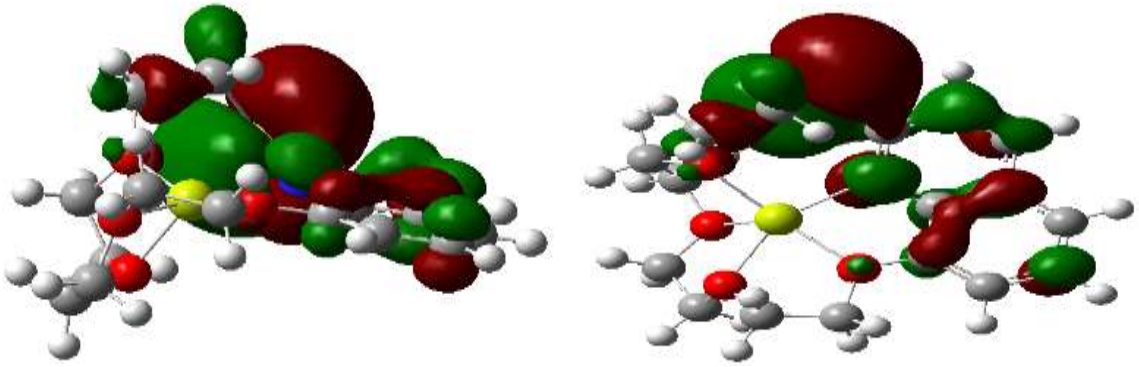

Figure 12: HOMO orbital of crown ether (L) and Mg^{2+} complex from two sides

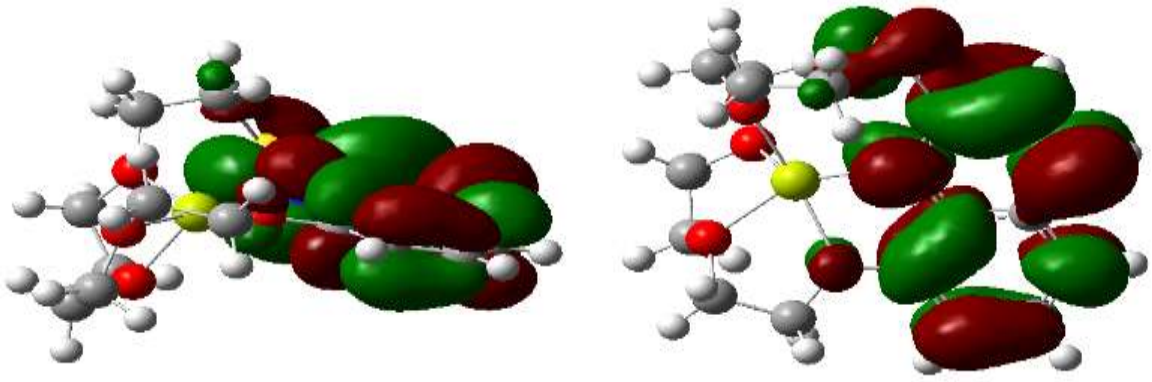

Figure 13: LUMO orbital of crown ether (L) and Mg^{2+} complex from two sides

Natural Bond Orbital Analysis (NBO)

NBO analysis provides an intensive tool for investigation of bonding, bonding interactions, charges on atoms and intramolecular and intermolecular charge delocalization in molecules and self-assembled systems. Thus, natural bond orbital analysis for **L**. Mg^{2+} complex was carried out; moreover, charges on atoms (Table 4) and interacting energies (E2) between donor (i) and acceptors (j) were reported (Table 5). E2 (i→j) is energy of delocalization and represents the charge transfer between donor (i) and acceptor (i) atoms. E2 of charge delocalization between donor and acceptor could be obtained using the following equation:

$$E2 = \Delta E_{ij} = q_i F^2(i,j) / (\varepsilon i - \varepsilon j)$$

In which, qi is equivalent to the donor orbital occupancy, εi and εj are diagonal elements (orbital energies) and F(i,j) are the off-diagonal elements of NBO Focks' matrix. The natural charges of heteroatoms in Mg^{2+} complex and crown (**L**) were obtained from NBO analysis is appeared in Table 4. According to Table 4, Mg^{2+} metal ion in corresponding complex has charge of 1.69095 e.

Table 4: Calculated NBO charges of L. Mg^{2+} complex

Atom	No	Natural Charge	Atom	No	Natural Charge
C	1	-0.20338	H	24	0.28087
C	2	-0.25351	H	25	0.26851
C	3	0.30929	H	26	0.27561
C	4	0.17004	H	27	0.29404
C	5	-0.09556	H	28	0.28384
C	6	-0.18426	H	29	0.26221
N	7	-0.72828	H	30	0.24153
C	8	0.16665	H	31	0.25403
C	9	-0.30917	H	32	0.26052
C	10	-0.06319	H	33	0.30422
S	11	0.27095	H	34	0.24646
O	12	-0.73129	H	35	0.25362
C	13	-0.09688	H	36	0.26187
C	14	-0.09141	H	37	0.23365
O	15	-0.75159	H	38	0.25836
C	16	-0.61105	H	39	0.24323
C	17	-0.07257	H	40	0.23757
O	18	-0.79026	H	41	0.26007
C	19	-0.09449	H	42	0.26090
C	20	-0.09339	H	43	0.26665
C	21	-0.08648	H	44	0.26384
C	22	-0.09651	Mg	45	1.69095
O	23	-0.76622			

E2, E(j)-E(i) and F(i,j) obtained from NBO analysis are reported in Table 5. According to Table 5, the strongest interactions are the intramolecular interactions of C-C bonds.

Table 5: NBO results of highest interactions between donors and acceptors for L.Mg^{2+} complex

Donor NBO (i)	Acceptor NBO (j)	E (2) kcal/mol	E(j)-E(i) a.u.	F (i, j) a.u.
C 9 - C 10	N 7 - C 8	70.58	0.41	0.155
C 2 - C 3	C 1 - C 6	93.01	0.04	0.115
C 4 - C 5	C 1 - C 6	80.58	0.06	0.116
C 4 - C 5	C 2 - C 3	286.65	0.02	0.119
C 4 - C 5	C 9 - C 10	103.39	0.05	0.115
N 7 - C 8	C 4 - C 5	77.21	0.07	0.101

Nuclear Independent Chemical Shifts (NICS) study

In order to investigate the effect of complex formation on aromaticity of pyridine and benzene moiety of quinolone, NICS (0) was calculated and reported in Table 6. According to NICS (0), no significant change was observed in aromaticity of crown and complexes.

Table 6: NICS (0) of crown and complexes for pyridine (P) and benzene moiety (B) of quinoline

Species	NICS (0), P	NICS (0), B
Crown (1) [b]	-6.5738	-9.1394
L.Li^{+} [a]	-6.1232	-9.3242
L.Na^{+} [a]	-5.8928	-9.7410
L.K^{+} [b]	-6.5876	-8.6004
L.Mg^{2+} [a]	-6.2280	-9.8454

a: HF/6-31g, b: HF/Lanl2DZ

Conclusions

The complex formation of quinoline aza oxa thia 17-crown-6 (**L**) with some metal cations (K^{+}, Na^{+}, Li^{+}, Mg^{2+}) has been studied theoretically. The calculations were conducted at the HF/6-31g and HF/Lanl2DZ levels of theory. According to the data obtained Mg^{2+} ion formed the most stable complex with crown and equilibrium binding constants of complex formation is: L. K^{+} < L. Na^{+} <L.Li^{+} <L.Mg^{2+}. The electron distribution over free crown and its L. Mg^{2+} complex was mainly over sulfur atom, using Highest Occupied Molecular Orbital (HOMO), and for both of them, Lowest Unoccupied Molecular Orbital (LUMO), were distributed over aromatic rings. HOMO and LUMO orbitals in L. Mg^{2+} complex was not distributed over Mg^{2+} ion and the ion are bare. Also, atomic charges and charge transfer between donors and acceptors in complex were studied using natural bond orbital analysis (NBO) and charge of Mg^{2+} ion in complex is 1.69095 e. Nuclear Independence Chemical Shift (NICS(0)) aromaticity for crown and complexes in two rings of quinoline (benzene and pyridine ring) were calculated and shows no significant change in aromaticity.

Acknowledgement

The financial support of this work by Payame Noor University (PNU) Research Council (Grant Number d/7/54093) is acknowledged.

References

1. (a) C.J. Pedersen, Synthesis and characterization of crown ethers, J. Am. Chem. Soc. 89 (1967) 7017-7036; (b) C.J. Pedersen, Crystalline salt complexes of macrocyclic polyethers, J. Am. Chem. Soc. 92 (1970) 386-391.

2. (a) K. Zhu, L. Wu, X. Yan, B. Zheng, M. Zhang, and F. Huang, Anion-Assisted Complexation of Paraquat by Cryptands Based on Bis (m-phenylene)-[32] crown-10, Chem. Eur. J. 16 (2010) 6088-6098; (b) Du, J.; Huang, Z.; Yu, X.-Q.; Pu, L. Highly selective fluorescent recognition of histidine by a crown ether–terpyridine–Zn (II) sensor, Chem. Commun. 49 (2013) 5399-5401.

3. (a) V. P. Boricha, S. Patra, Y. S. Chouhan, P. Sanavada, E. Suresh, P. Paul, Synthesis, Characterisation, Electrochemistry and Ion-Binding Studies of Ruthenium (II) and Rhenium (I) Bipyridine/Crown Ether Receptor Molecules, Eur. J. Inorg. Chem. (2009) 1256-1267; (b) H. Sharghi, R. Khalifeh A. R. S. Beni, Synthesis of new lariat ethers containing polycyclic phenols and heterocyclic aromatic compound on graphite surface via mannich reaction, J. Iran. Chem. Soc. 7 (2010) 275-288.

4. (a) K. Zhu, L. Wu, X. Yan, B. Zheng, M. Zhang, and F. Huang, Anion-Assisted Complexation of Paraquat by Cryptands Based on Bis (m-phenylene) - [32] crown-10. Chem. Eur. J. 16 (2010) 6088-6098; (b) L.F. Lindoy, New super-and supramolecular receptor systems-cages, chains, squares and dendrimers incorporating macrocycles as structural elements, J. Iran. Chem. Soc. 1 (2004) 1-9.

5. (a) U.H.F. Bunz, Y. Rubin, Tobe, Y. Polyethynylated cyclic π-systems: scaffoldings for novel two and three-dimensional carbon networks. Chem. Soc. Rev. 28 (1999) 107-119; (b) J.S. Moore, Shape-persistent molecular architectures of nanoscale dimension. Acc. Chem. Res. 30 (1997) 402-413; (c) E. Mattia, S. Otto, Supramolecular systems chemistry, Nature Nanotechnol. 10 (2015) 111-119.

6. C.M. Hong, R.G. Bergman, K.N. Raymond and F.D. Toste, Self-assembled tetrahedral hosts as supramolecular catalysts. *Acc. Chem. Res.*, 51 (2018) 2447-2455.

7. T. Jiang, X. Wang, J. Wang, G. Hu, X. Ma, Humidity-and Temperature-Tunable Multicolor Luminescence of Cucurbit [8] uril-Based Supramolecular Assembly. *ACS Appl. Mater.Interfaces*, 11 (2019) 14399-14407.

8. (a) J.-M. Lehn, J.L. Atwood, J.E.D. Davies, D.D. McNicol, F. Vögtle, D.N. Reinhoudt, In *Comprehensive Supramolecular Chemistry*; Pergamon: Oxford, 1996; Vol. 10; (b) Q.X. Geng, F. Wang, H. Cong, Z. Tao, G. Wei, Recognition of silver cations by a cucurbit [8] uril-induced supramolecular crown ether, *Org. Biomol. Chem.* 14 (2016) 2556-2562.

9. J. P. Majoral, A. M. Caminade, Phosphorhydrazones as Useful Building Blocks for Special Architectures: Macrocycles and Dendrimers. *Eur. J. Inorg. Chem.*, *2019*, (2019) 1457-1475.

10. (a) W. Zhang, Y.-M. Zhang, S.-H. Li, Y.-L. Cui, J. Yu, Y. Li, Tunable Nanosupramolecular Aggregates Mediated by Host–Guest Complexation, *Angew. Chem.* 128 (2016) 11624-11628; (b) Y.Q. Yao, K. Chen, Z.Y. Hua, Q.J. Zhu, S.F. Xue, Z. Tao, Cucurbit [n] uril-based host–guest-metal ion chemistry: an emerging branch in cucurbit [n] uril chemistry, *J. Incl. Phenom. Macrocycl. Chem.* (2017) 1-4.

11. X.Y. Lou, Y.P. Li, Y.W. Yang, Gated Materials: Installing Macrocyclic Arenes-Based Supramolecular Nanovalves on Porous Nanomaterials for Controlled Cargo Release. *Biotechnology journal*, *14* (2019), 1800354.

12. L. Türker, Interaction of *Trans*-Retinol And 1,1-Diamino-2,2-Dinitroethylene (FOX-7)-A DFT Treatment, *To Chem. J.*, 3 (2019) 85-96.

13. (a) E. Rostami, Synthesis of New 1-Naphthol Aza Oxa Thia Crowns, *Phosphorus, Sulfur Silicon Relat. Elem*. 186 (2011) 1694-1701; (b) E. Rostami, Efficient Route for the Synthesis of New Dinaphthosulfoxide Aza Crowns Using Ethyleneglycol under Microwave (MW) Irradiation: Macrocyclization is Preferred to Oligomerization under MW Irradiation. *Phosphorus, Sulfur Silicon Relat. Elem*. 186 (2011) 1853-1866; (c) E. Rostami, M. Ghaedi, M. Zangooei, A. Zare, Synthesis of new aza thia crowns under microwave irradiation. *J. Sulfur Chem*. 33 (2012) 327-333; (d) M. Taghdiri, E. Rostami, Preparation and characterization of organic–inorganic adduct of dinaphtosulfide macrocyclic diamide and silicotungstic acid: study of interaction in solid and solution phase. *J. Sulfur Chem*. 36 (2015) 270-280.

14. Gaussian 09, Revision E.01, M. J. Frisch, G. W. Trucks, H. B. Schlegel, G. E. Scuseria, M. A. Robb, J. R. Cheeseman, G. Scalmani, V. Barone, B. Mennucci, G. A. Petersson, H. Nakatsuji, M. Caricato, X. Li, H. P. Hratchian, A. F. Izmaylov, J. Bloino, G. Zheng, J. L. Sonnenberg, M. Hada, M. Ehara, K. Toyota, R. Fukuda, J. Hasegawa, M. Ishida, T. Nakajima, Y. Honda, O. Kitao, H. Nakai, T. Vreven, J. A. Montgomery, Jr., J. E. Peralta, F. Ogliaro, M. Bearpark, J. J. Heyd, E. Brothers, K. N. Kudin, V. N. Staroverov, R. Kobayashi, J. Normand, K. Raghavachari, A. Rendell, J. C. Burant, S. S. Iyengar, J. Tomasi, M. Cossi, N. Rega, J. M. Millam, M. Klene, J. E. Knox, J. B. Cross, V. Bakken, C. Adamo, J. Jaramillo, R. Gomperts, R. E. Stratmann, O. Yazyev, A. J. Austin, R. Cammi, C. Pomelli, J. W. Ochterski, R. L. Martin, K. Morokuma, V. G. Zakrzewski, G. A. Voth, P. Salvador, J. J. Dannenberg, S. Dapprich, A. D. Daniels, Ö. Farkas, J. B. Foresman, J. V. Ortiz, J. Cioslowski, and D. J. Fox, Gaussian, Inc., Wallingford CT, 2009.

15. GaussView, Version 5, Roy Dennington, Todd Keith, and John Millam, *Semichem Inc*., Shawnee Mission, KS, 2009.

16. L. Yue, P. Wustelt, A.M. Sayler, F. Oppermann, M, Lein, G.G. Paulus, S. Gräfe, Strong-field polarizability-enhanced dissociative ionization. *Phys. Rev. A*, 98 (2018) 043418.

17. P. Bhattacharya, R.R. Das, R.S. Katiyar, Fabrication of stable wide-band-gap ZnO/MgO multilayer thin films. *Appl. Phys. Lett.*, 83 (2003) 2010-2012.

18. F. De Proft, N. Sablon, D.J. Tozer, P, Geerlings, Calculation of negative electron affinity and aqueous anion hardness using Kohn–Sham HOMO and LUMO energies. *Faraday Discuss.*, 135 (2007) 151-159.